IOP Conf. Series: Journal of Physics: Conf. Series **1224** (2019) 012037 doi:10.1088/1742-6596/1224/1/012037

Design and assessment of an experimental facility for the characterization of flow boiling of azeotropic refrigerants in horizontal tubes

Luigi Pietro Maria COLOMBO*, Andrea LUCCHINI*, Thanh Nhan PHAN*, Luca MOLINAROLI*, Alfonso NIRO*

* Dipartimento di Energia (Politecnico di Milano, via Lambruschini 4, 20156, Milano)

luigi.colombo@polimi.it

Abstract. An experimental facility was designed to measure pressure drop and heat transfer coefficient during flow boiling of azeotropic refrigerants in horizontal tubes. The apparatus is made of the refrigerant circuit, including the test section; the water circuit, to provide the power for evaporation; the glycol-water circuit, to fix the refrigerant pressure. The test section is a counterflow tube-in-tube heat exchanger (refrigerant inside, water outside). Plant assessment involved the measurement of pressure drop and heat transfer during R134a flow boiling in a smooth tube (outer diameter 9.56mm, inner diameter 8.92mm). Such a case study is a benchmark for the availability of a wide experimental database in the literature, which has been also summarized in many correlations. Then further tests involved a microfin tube. The experimental conditions were: evaporation temperature, 5°C; mass flux, 111÷333kg/m^{2}s; average quality, 0.15÷0.93; heat flux, 8.8kW/m^2 and 17.6kW/m^2. The uncertainty affecting the pressure drop and the heat transfer coefficient resulted lower than 1% and 5% respectively. The comparison with the literature shows satisfactory agreement with the major findings and enables using the data for the assessment of the existing models to predict both the pressure drop and the heat transfer coefficient.

1. Introduction

HVAC technologies are continually evolving to meet more and more severe requirements in terms of energy efficiency and environmental impact. The related heat transfer processes represent very often the bottleneck on improving the overall performance. In particular, if phase transitions are involved, the uncertainties related to the complex behavior of multiphase flows may significantly affect the design of a refrigeration system. A thorough characterization of boiling and condensation processes is then required to endow engineers with more and more accurate design tools.The task becomes more difficult if the smooth tube is replaced by a microfin tube. Many authors keep on working on this topic to provide experimental data [1, 2, 3, 4, 5, 6, 7] and correlations [8, 9, 10]. Accordingly, an experimental facility was designed to measure the pressure drop and the heat transfer coefficient during flow boiling of azeotropic refrigerants in horizontal tubes.Plant assessment involved the measurement of pressure drop and heat transfer during flow boiling of R134a in a smooth tube. The following step concerned the study of a microfin tube.

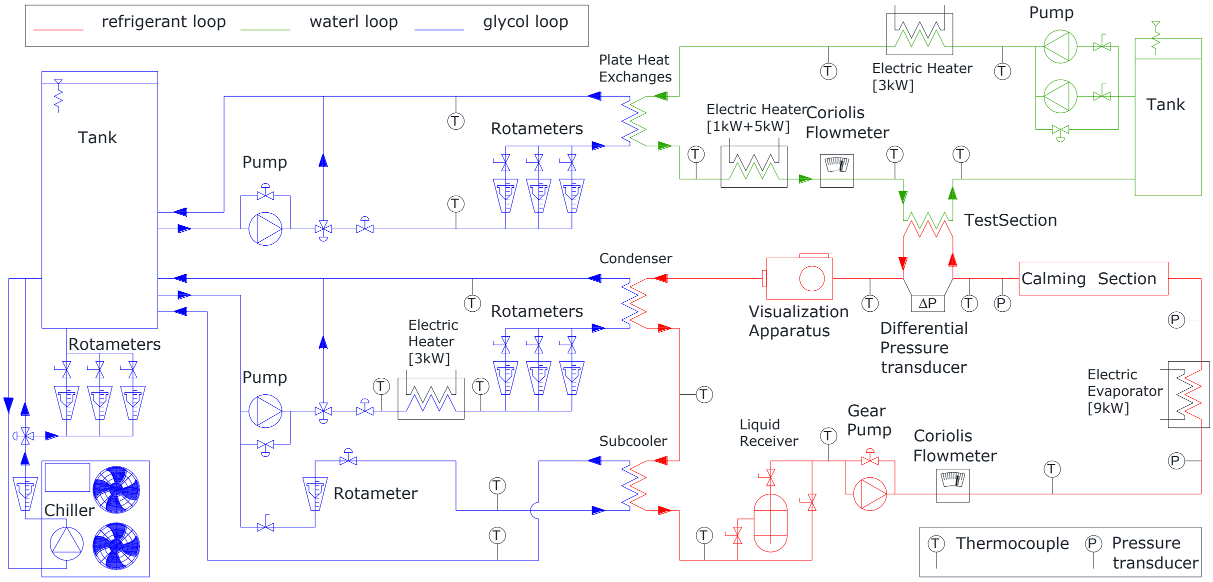

Figure 1. Experimental apparatus scheme.

2. Experimental apparatus

The experimental apparatus (Figure 1), is made of three main circuits named: the refrigerant loop (filled with R134a), the water loop (filled with demineralized water) and glycol loop (filled with a mixture of water and ethylene glycol, 30% volume concentration). They exchange thermal power each other in order to set the test condition and perform the experiments.

2.1. *The glycol loop*

The glycol loop (blue line in Figure 1) is a service circuit with two main tasks: to set the operating temperature in the test section (fixing the pressure in the condenser) and to chill both refrigerant and water. A commercial chiller (21kW cooling capacity) cools the mixture to -10°C and then it is stored in a 0.75m^3 tank. Two independent loops, one for the water and the other for therefrigerant, are connected to the tank.

The loop dedicated to the water cools down the water entering in the test section, which heats up as a consequence of the viscous dissipation.

The other loopis in charge to set the temperature in the test section and to prevent cavitation in the refrigerant pump. The former operation is accomplished setting the mass flow rate, using a manual needle valve, and the temperature (checked by a K-type thermocouple) at the condenser inlet, using a P.I.D. driven electric heater (3kW), such that the refrigerant pressure at the test section inlet (which is the sum of the pressure in the condenser and the pressure drop in between) be the saturation pressure corresponding to the test temperature. For the latter operation a bypass drains part of the cold mixture headed to the electric heater (the volume flow rate is tuned using a manual needle valve) to subcool the liquid refrigerant entering the pump.

2.2. *The water loop*

The water loop (green line in Figure 1) is designed to exchange the thermal power required for the refrigerant phase change. The heat transfer takes place in a tube-in-tube heat exchanger (water in the annulus, refrigerant in the inner duct), named test section (Figure 2), thermally insulated from the surroundings with 100 mm thick shell of rubber foam. A pump drains the water from the tank (thermally insulated with a Rockwool shell 5cm thickness, volume 0.2m^3), a bypass and a manual needle valve fix the mass flow rate, its value is measured by a Coriolis flowmeter (range [0;400]kg/h, uncertainty 0.15% of the reading). Afterwards a K-type thermocouple checks the water temperature

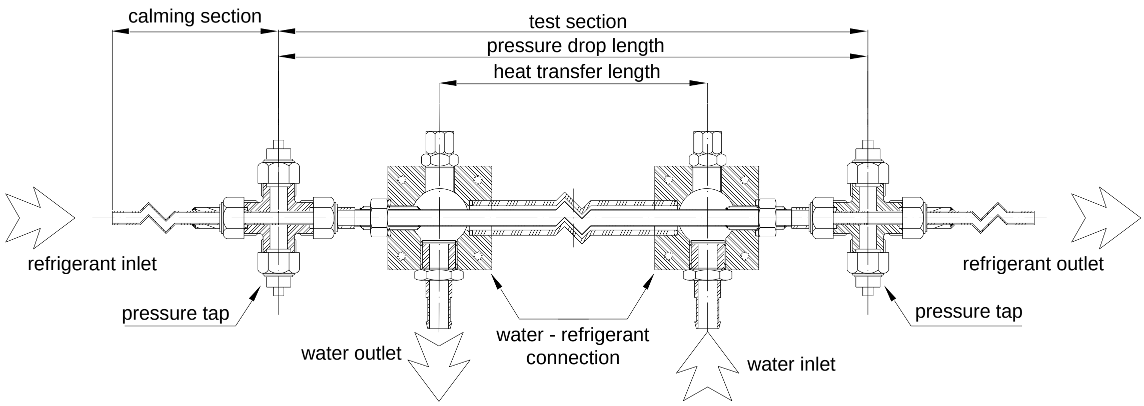

Figure 2. Test section.

and the flowenters in a plate heat exchanger (if cooling is required glycol is flushed in the other side), then an P.I.D. driven electric heater (it is made of two elements: 1kW and 5kW, it is possible to use both or only one) sets the inlet temperature in the test section (checked by a K-type) such that the power transfer causes a ±2°C temperature change of the water flow (inlet and outlet temperature are provided by two groups of 3 K-type thermocouples connected in series, uncertainty 0.1K). Finally the water returns to the tank.

2.3. *The refrigerant loop*

The main goal of the refrigerant loop (red line in Figure 1) is to provide a two phase flow of refrigerantat the operating conditions (which are defined by the mass flow rate, the inlet quality and the inlet temperature), at the inlet of the test section, where the measures take place.

A saturated liquid flow of refrigerant leaves the condenser (four plate heat exchanges and one shell end tube heat exchanger in parallel, depending on the thermal duty it is possible to use one or more of them) and enters in a plate heat exchanger (subcooler) to be chilled and to prevent cavitation in the circulation pump (gear type with inverter driven engine for the mass flow rate tuning). A Coriolis flowmeter (range [0;400]kg/h, uncertainty 0.15% of the reading) records the mass flow rate while a pressure transducer (relative, range [-1;30]bar, uncertainty ±1% of full scale) and a thermocouple (K-type, uncertainty 0.1K) check the thermodynamic state of the refrigerant as it enters in the evaporator (it is a set of 8 electric heaters, 9kW total power, driven by a software control system) which provides the power to vaporize the amount of refrigerant specified by the test section inlet quality. A straight duct (4.7 m long adiabatic duct and thermally insulated by a 5cm thick rubber foam shell), designed for the development of the two phase flow regime, is placed before the test section. Then the refrigerant enters in the test section, the visualization apparatus, for the recording and identification of the flow pattern, followsand, in the end, the refrigerant returns to the condenser.

The test section (Figure 2) is a tube in tube heat exchanger (heat transfer length L=1.11m)

Table 1. Microfin tube characteristics

Tube type			J60	smooth
inner diameter (fin root)	D_r	[mm]	8.96	8.92
outer diameter	D	[mm]	9.52	9.52
wet perimeter	S_p	[mm]	44.9	28.0
cross section area	A_c	[mm^2]	62.1	62.5
hydraulic diameter	D_h	[mm]	5.28	8.92
exchanging area ratio			1.68	1
fin number	n	[N]	60	
height	H	[mm]	0.2	
apex angle	α	[°]	40	
helix angle	β	[°]	18	

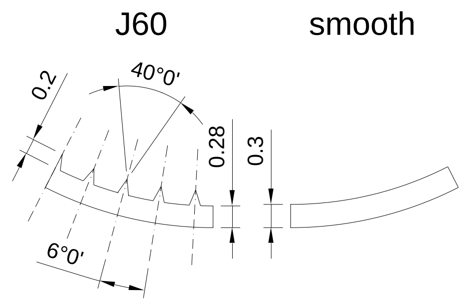

Figure 3. Microfin tube geometric characteristics

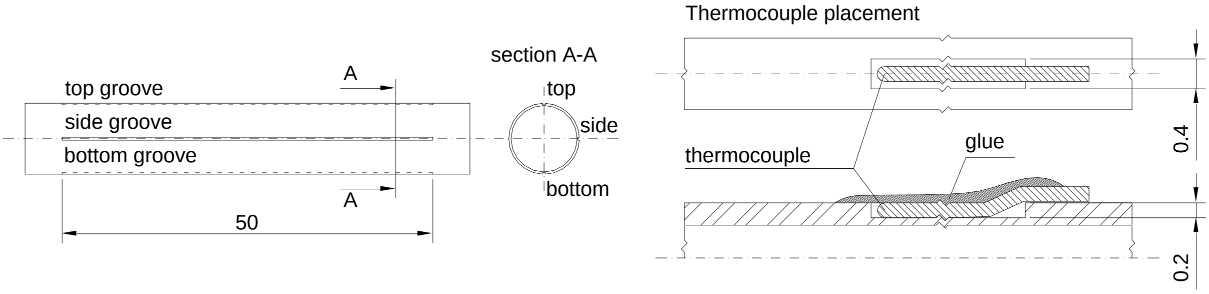

Figure 4. Thermocouple and grooves positions.

thermally insulated with 10 cm thick rubber foam shell. As different geometries are available for the inner surface of the refrigerant duct, the smooth tube is the reference to compare the microfin tube. Their geometrical characteristics are reported in Table 1 while Figure 3 shows the main differences.

To record the pressure drop a differential pressure transducer (range [-1.0;1.0]bar, uncertainty ±0.1% of the full scale), connected to two pressure taps (separated by a distance of L_p=1.3m), is used. A relative pressure transducer (range [-1;16]bar, uncertainty ±0.25% of the full scale), connected to the tap at the inlet of the test section, reads the refrigerant pressure. The refrigerant inlet and outlet temperatures are the saturation temperatures given by the pressure readings. Two groups (one at the entrance and one at the exit) of three thermocouples are glued inside grooves (length 50mm, depth 0.15mm, width 0.4mm) on the outside on the inner tube (top, side and bottom position), to measure the wall temperatures (Figure 4). The reference junction of each thermocouple (K-type, uncertainty 0.1K) is inserted in a Dewar flask filled with melting ice.

3. Data reduction

All the measuring devices are connected, via an acquisition board, to a computer which is endowed of a program to read and to store their signals. As the data acquisition ends another program performs the post processing to compute the quantities that identify the experimental operating conditions (refrigerant mass flux G, quality change in the test section Δx, average quality in the test section x_m), the pressure drop per unit length $\Delta P/L_p$ and the heat transfer coefficient h. One data point is obtained for each experimental condition, averaging 12 acquisitions; each of them is the mean value of the readings recorded during a time interval of 180s. As the sampling frequency is 1Hz, 181 samples are stored during each acquisition. Preliminary experiments were performed on single phase vapor flow to check the data acquisition and the post-processing. The results showed an agreement within ±5% with the most commonly used correlations for both heat transfer and pressure drop.

Referring to the microfin tube nominal geometrical characteristics, the net cross section area is:

$$A_c = \frac{\pi D_r^2}{4} - \frac{nH^2}{\cos(\beta)} tg\left(\frac{\alpha}{2}\right) \tag{1}$$

From the Coriolis flowmeter reading the refrigerant mass flux is computed as follows:

$$G = \frac{\dot{m}_r}{A_c} \tag{2}$$

Assuming steady state and negligible the thermal dispersion in the test section, power transfer takes place only between water and refrigerant:

$$Q = \dot{m}_a c_{pa}(T_{ai} - T_{ao}) \tag{3}$$

The quality change can be computed as:

$$\Delta x = (x_o - x_i) = \frac{\dot{Q}}{\dot{m}_r h_{lv}(p_r)} \tag{4}$$

The inlet quality can be computed performing an energy balance on the evaporator, assuming steady state and negligible thermal dispersion:

$$x_i = \frac{Q_e - \dot{m}_r c_{pr}[T_s(p_r) - T_{ri}]}{\dot{m}_r h_{lv}(p_r)} \tag{5}$$

In the end the mean quality in the test section is:

$$x_m = x_i + \frac{\Delta x}{2} \tag{6}$$

The pressure drop per unit length is immediately computed as the distance L_p between the pressure taps at the edges of the test section is known and the total (frictional and accelerative) pressure drop Δp is measured by a differential pressure transducer.

For the average heat transfer coefficient h in the test section a longer procedure is required. As it is based on the logarithmic mean temperature between wall and refrigerant at first temperatures are required. As three thermocouples read the wall temperature, both at the inlet and at the outlet of the refrigerant, their readings are averaged to get a single value for the wall temperature.

$$T_w = \frac{T_t + T_s + T_b}{3} \tag{7}$$

The inlet and outlet refrigerant temperatures are the saturation temperatures corresponding to the inlet (measured by a relative pressure transducer) and the outlet pressure (computed subtracting the pressure drop on the test section to the inlet pressure).

$$T_r = T_{sat}(p) \tag{8}$$

It follows that the logarithmic mean temperature difference is:

$$\Delta T_{ml} = \frac{(T_{wo} - T_{ro}) - (T_{wi} - T_{ri})}{ln \frac{T_{wo} - T_{ro}}{T_{wi} - T_{ri}}} \tag{9}$$

The heat transfer area of the refrigerant duct is referred to the fin rootdiameter, hence the average heat transfer coefficient in the test section is given by the following equation:

$$h = \frac{Q}{\pi D_r L \Delta T_{ml}} \tag{10}$$

Uncertainty analysis showed that the logarithmic mean temperature difference has the largest influence on the average heat transfer coefficient uncertainty. For instance, Figure 5 shows the behaviour for experiments at Q=288W (relative uncertainty 2.5%), L=1.11m (relative uncertainty 1.4%), D_r=8.96mm (the nominal fin root diameter is considered uncertainty free); for temperature readings the uncertainty is U_T=0.1K. The chart shows that, even if a single measure has a very large uncertainty (it is never lower than 3%), the average value of a single acquisition proves to be lower than 5% for all the experimental operating conditions. The same test was repeated for all the operating conditions and the same outcome followed.

4. Experimental results

The experimental conditions were identified by four quantities: the refrigerant inlet temperature in the test section, T_{ri}=5°C; the refrigerant mass flux, G ranges in the interval [110;334]kg/m^{2}s; the mean quality, x_m ranges in the interval [0.15;0.95], the heat flux referred to the fin root surface of the microfin tube, q_1=8.6kW/m^2 and q_2=2q_1=17.2kW/m^2.Heat flux values were chosen such that the quality change Δx in the test section ranges from 0.06 to 0.2.

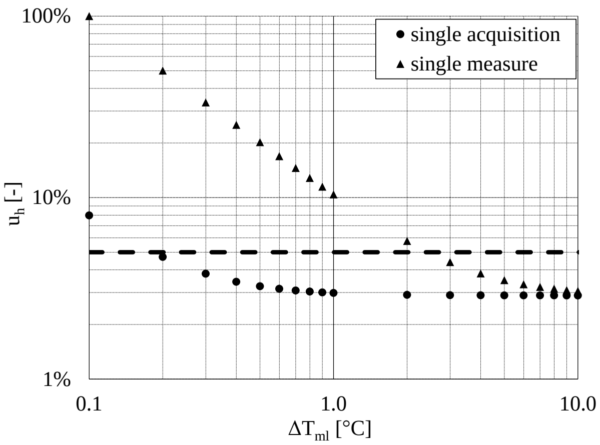

Figure 5. Average heat transfer coefficient relative uncertainty.

4.1. Smooth tube

Figure 6 reports the pressure drop per unit length for all the operating conditions tested using the smooth tube. As expected as the mass flux grows the pressure drop increases on the contrary the influence of heat flux seems to be negligible. As the mean quality increases (0.15<x_m<0.85) pressure drop grows then

($0.85<x_m<0.90$) a maximum is reached and finally ($0.85<x_m<0.95$) pressure drop falls off toward the data point for the only vapour phase pressure drop.

The heat transfer coefficient h (Figure 7) is mainly affected by the heat flux, as the latter increases the former does the same. Similar is the effect of the mass flux on the heat transfer coefficient, as the mass flux grows the heat transfer coefficient increases too.

In the end is it possible to observe, as expected, that the heat transfer increases as the mean quality increases as long as the thermal crisis takes place (x_m in the range [0.80;0.95]), then a very steep reduction of the heat transfer coefficient can be observed.

4.2. Microfin tube

For the microfin tube the effect of the heat flux, the mass flux and the mean quality on the pressure drop per unit length is the same described for the smooth tube.The only difference, as can be observed from Figure 8, is that pressure drop is larger for microfin tube, as a consequence of the fin presence.

As the heat flux increases the heat transfer coefficient h grows (Figure 9).About the connection between mass flux and heat transfer coefficienta difference, between smooth and microfin tube, can be observed.From the chartin Figure 9 two main comments arise: at low mass flux values the heat transfer coefficient raises as the mass flux grows; at high mass flux values the heat transfer coefficient is independent of mass flux. That behavior could be related to a flow regime transition from stratified flow to annular flow.In the end is it possible to observe, as expected, that the heat transfer increases as the mean quality increases, moreover the microfin tube seems to be very effective in keeping the liquid in touch with the whole perimeter of the tube because no thermal crisis was observed.

5. Comparison between experimental data and correlations

The comparison between the experimental data and the correlation prediction (reported only for the microfin tube for space constraint) is performed computing the average percentage error E and the standard deviation σ of E.

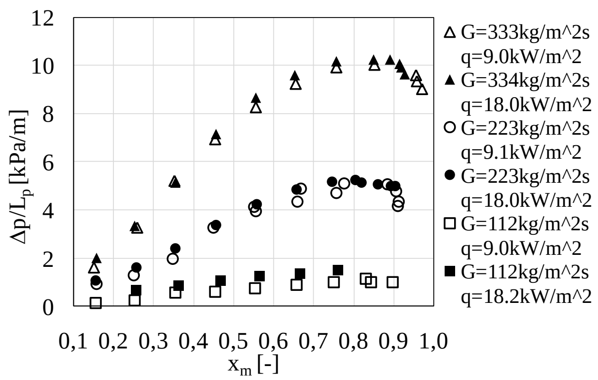

Figure 6. Pressure drop, smooth tube.

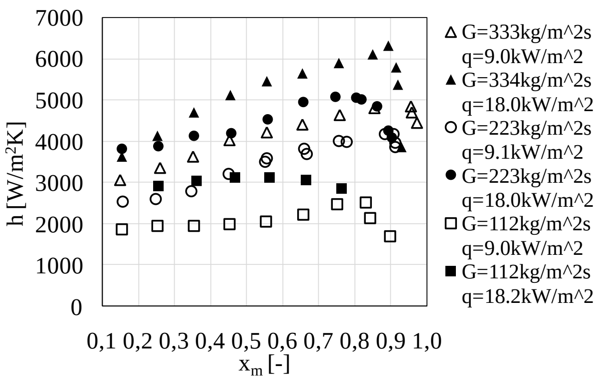

Figure 7. Heat transfer coefficient, smooth tube.

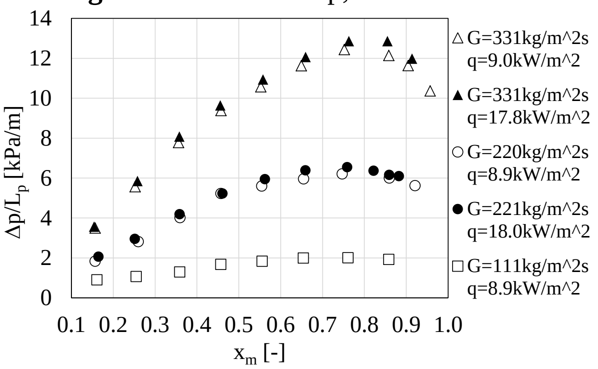

Figure 8. Pressure drop, microfin tube.

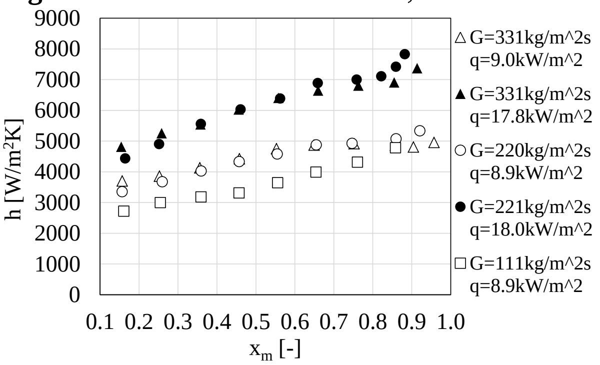

Figure 9. Heat transfer coefficient, microfin tube.

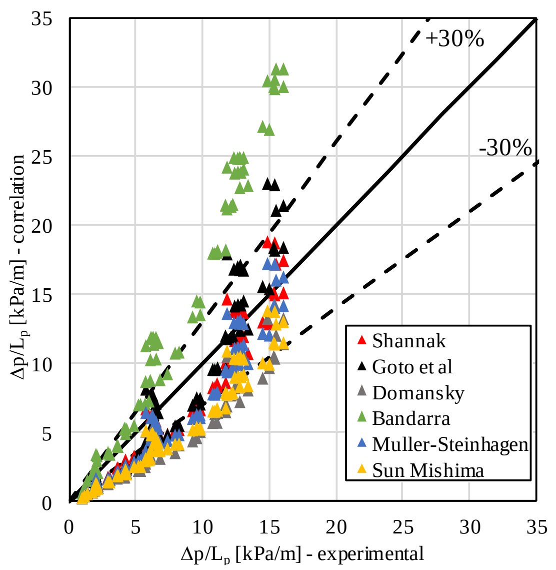

Figure 10. Pressure drop per unit length.

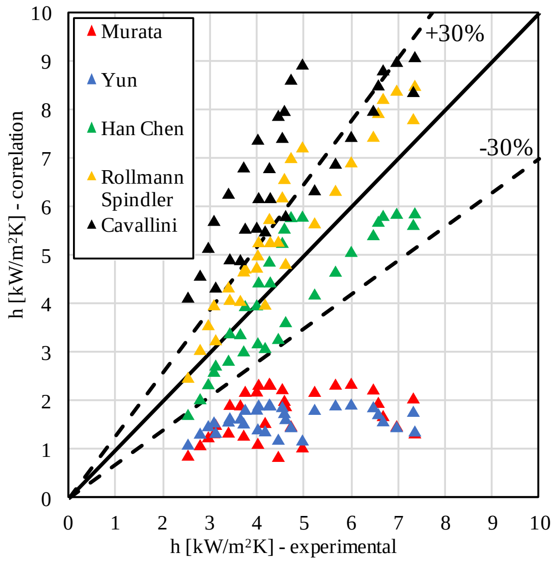

Figure 11. Heat transfer coefficient.

$$E = \frac{1}{N}\sum_{j=1}^{N}\frac{x_{j,c} - x_{j,e}}{x_{j,e}} \tag{11}$$

As reported in Table 2 and Figure 10, the majority of the correlation for pressure drop checked, but Bandarra, underestimates the experimental data. Goto et al. is the correlation with the smallest percentage error, but its standard deviation is large, and it seems unable to properly describe the trend of the pressure drop. On the contrary Sun-Mishima's and Domansky's have the smallest standard deviation but very large percentage errors, meaning that a further calibration of the parameters is required.

Table 3 and Figure 11 shows that, concerning heat transfer, the Yun's and Murata's correlations largely underestimates the data, while Cavallini's does the opposite. Han-Chen correlation shows a better agreement with the data, it has the smallest error, but the largest standard deviation.

6. Conclusions

It is known that the microfin tube exhibits a significant heat transfer enhancement, when compared to the smooth tube, butpressure drop increases as well. The experimental data shows that the latter increases slightly more (9%). Comparison between the predictions of various correlations from literature andexperimental data both on heat transfer and pressure drop was proposed. The best resultsfor the heat transfer are achieved by the Han Chen scheme of correlation, whereas, for the pressure drop, it seems that the influence ofgeometry is still not completely described in the models considered.

Acknowledgments

The financial support of MIUR through the program PRIN 2015 (Grant Number 2015M8S2PA) is greatly acknowledged. The authors thank Fabio Pulcini for the aid in taking measurement.

Table 2. Pressure drop

Correlation	E	σ
Shannak	-24%	21%
Muller-Steinhagen	-27%	20%
Bandarra	55%	34%
Sun Mishima	-39%	14%
Domansky	-41%	15%
Goto et al	-14%	31%

Table 3. Heat transfer coefficient

Correlation	E	σ
Murata	-53%	15%
Yun	-61%	9%
Han Chen	12%	32%
Rollmann Spindler	33%	22%
Cavallini	53%	25%

IOP Conf. Series: Journal of Physics: Conf. Series **1224** (2019) 012037 doi:10.1088/1742-6596/1224/1/012037

Nomenclature: Latin symbols

A_c	cross section area [m^{-2}]
c_{pa}	water specific heat capacity [$J\cdot kg^{-1}\cdot K^{-1}$]
c_{pr}	refrigerant specific heat capacity [$J\cdot kg^{-1}\cdot K^{-1}$]
D	outer diameter [m]
D_h	hydraulic diameter [m]
D_r	inner diameter (fin root) [m]
E	mean percentage error [-]
G	refrigerant mass flux [$kg\cdot m^{-2}\cdot s^{-1}$]
H	fin height [m]
h	heat transfer coefficient [$W\cdot m^{-2}\cdot K$]
h_{lv}	liquid vapour enthalpy of phase change [$J\cdot kg^{-1}$]
L	heat transfer length [m]
L_p	distance between the pressure taps [m]
$\dot{m}_a$	water mass flow rate [$kg\cdot s^{-1}$]
$\dot{m}_r$	refrigerant mass flow rate [$kg\cdot s^{-1}$]
n	fin number
p_r	refrigerant pressure [Pa]
Q	power exchanged in the test section [W]
Q_e	power provided by the electric evaporator [W]
S_p	wet perimeter [m]
T_{ai}	water inlet temperature [K]
T_{ao}	water outlet temperature [K]
T_b	temperature in the bottom position [K]
T_{ri}	refrigerant inlet temperature [K]
T_{ro}	refrigerant outlet temperature [K]
T_s	temperature in the side position [K]
T_t	temperature in the top position [K]
T_{wi}	mean wall temperature, refrigerant inlet [K]
T_{wo}	mean wall temperature, refrigerant outlet [K]
x_i	refrigerant inlet quality [-]
$x_{j,c}$	correlation value [-]
$x_{j,e}$	experimental value [-]
x_m	average quality in the test section [-]

Nomenclature: Greek symbols

α	apex angle [°]
β	helix angle [°]
Δp	pressure drop [Pa]
ΔT_{ml}	log mean temperature difference [K]
Δx	quality change [-]
σ	standard deviation [-]

References

[1] Bandarra Filho E P, Saiz Jabardo J M, EL Barbieri P, 2004 Convective boiling pressure drop of refrigerant R-134a in horizontal smooth and microfin tubes. *International journal of refrigeration* **27(8)** 895–903

[2] Shannak B A, 2008 Frictional pressure drop of gas liquid two-phase flow in pipes. *Nuclear Engineering and Design* **238(12)** 3277–3284

[3] Han X H, Fang Y B, Wu M, Qiao X G, Chen G M, 2017 Study on flow boiling heat transfer characteristics of R161/oil mixture inside horizontal micro-fin tube. *International Journal of Heat and Mass Transfer* **104** 276–287

[4] Rollmann P, Spindler K, Muller-Steinhagen H, 2011 Heat transfer, pressure drop and flow patterns during flow boiling of R407c in a horizontal microfin tube. *Heat and mass transfer* **47(8)** 951-958

[5] Cavallini A, Del Col D, Mancin S, Rossetto L, 2009 Condensation of pure and near-azeotropic refrigerants in microfin tubes: A new computational procedure. *International Journal of Refrigeration* **32(1)** 162–174

[6] Colombo L P M, Lucchini A, Muzzio A, 2012 Flow patterns, heat transfer and pressure drop for evaporation and condensation of R134a in microfin tubes *International Journal of Refrigeration* **35(8)** 2150–2165

[7] Goto M, Inoue N, Ishiwatari N, 2001 Condensation and evaporation heat transfer of R410a inside internally grooved horizontal tubes. *International Journal of Refrigeration* **24(7)** 628–638

[8] Sun L, Mishima K, 2009 Evaluation analysis of prediction methods for two-phase flow pressure drop in mini-channels. *International Journal of Multiphase Flow* **35(1)** 47–54

[9] Muller-Steinhagen H, Heck K, 1986 A simple friction pressure drop correlation for two-phase flow in pipes. *Chemical Engineering and Processing: Process Intensification* **20(6)** 297–308

[10] Xu Y, Fang X, Su X, Zhou Z, Chen W, 2012, Evaluation of frictional pressure drop correlations for two-phase flow in pipes. *Nuclear Engineering and Design* **253** 86-97